Journal of Theoretical and Applied Vibration and Acoustics 10(2) 23-33 (2024)

I S A V

Journal of Theoretical and Applied Vibration and Acoustics

journal homepage: http://tava.isav.ir

A parametric optimization of vortex bladeless generator

Seyed Saeid Mansouri[a], Mohammad Reza Elhami [*,b], Rouhollah Hosseini[c]

[a] *Ph.D. Candidate, Mechanical Engineering Faculty, Imam Hossein Comprehensive University, Tehran, Iran*
[b] *Associate Professor, Mechanical Engineering Faculty, Imam Hossein Comprehensive University, Tehran, Iran*
[c] *Assistant Professor, Mechanical Engineering Faculty, Imam Hossein Comprehensive University, Tehran, Iran*

Research Article

A R T I C L E   I N F O

Article history:
Received 15 March 2024

Received in revised form
15 August 2024

Accepted 27 August 2024

Available online 19 November 2024

Keywords:
Bladeless generator

Optimization

Mass-damping parameter

A B S T R A C T

A vortex-bladeless turbine is a device that works with vortex-induced vibration, which is generated by wind energy. It is one of the innovative devices for wind energy harvesting with some remarkable advantages compared to classical turbines. Such wind turbines have numerous advantages, including less maintenance than classical windmills, lower manufacturing costs, and easier installation. Vortex's nobility comes from its spectacular form of harvesting energy by vibration. The mast vibrates in the wind, with lift force made with Von-Karman vortices when a moving air cross-passes over a mast (with a mean diameter of the mast **D**) structure. At the lower part of the mast, an elastic rod (carbon fiber) moves an alternator and harvests electricity with the least parts in contact. To optimize this technology for harvesting the potential energy, one of the critical parameters is the mean diameter D, which is analytically studied to have the largest displacement amplitude at the tip of the mast. To this end, the bladeless generator is simulated as a one-degree-of-freedom system moving transverse with the flow direction. The mass-damping parameter (m*ζ), which depends on a mast and core fabric, is investigated. Air forces are extracted from experimental experiences, and fabrics are determined at the design stage according to references (carbon fiber for the core and carbon glass for the mast). The velocity of the air is determined according to where the bladeless generator will be installed. In the end, the results are verified by CFD methods in fluent software. ICEM software is used for meshing the 2-dimensional model. The Piso algorithm and kω-sst model are applied to model the airflow to solve the problem.

1. Introduction

Vortex Bladeless Generators (Figure 1.) create a windmill (mast) with no rotating parts like gears or shafts. This device is a new way of harvesting wind energy that inspires and develops the wind harvesting market. The Vortex device is made of a mast that oscillates in the low-range velocity of wind and generates energy as it moves. The vortices are generated according to vortex-shedding theory, and the turbine converts the kinetic energy of the air into electrical energy using an

[*] Corresponding author:
E-mail address: mrelhami.63@gmail.com (M.R. Elhami)

http://dx.doi.org/10.22064/tava.2024.2024948.1235

electromagnetic alternator or piezoelectric mechanism. This phenomenon occurs in a steady and unsteady airflow for a specific range of Reynolds numbers, as shown in Figure 2.

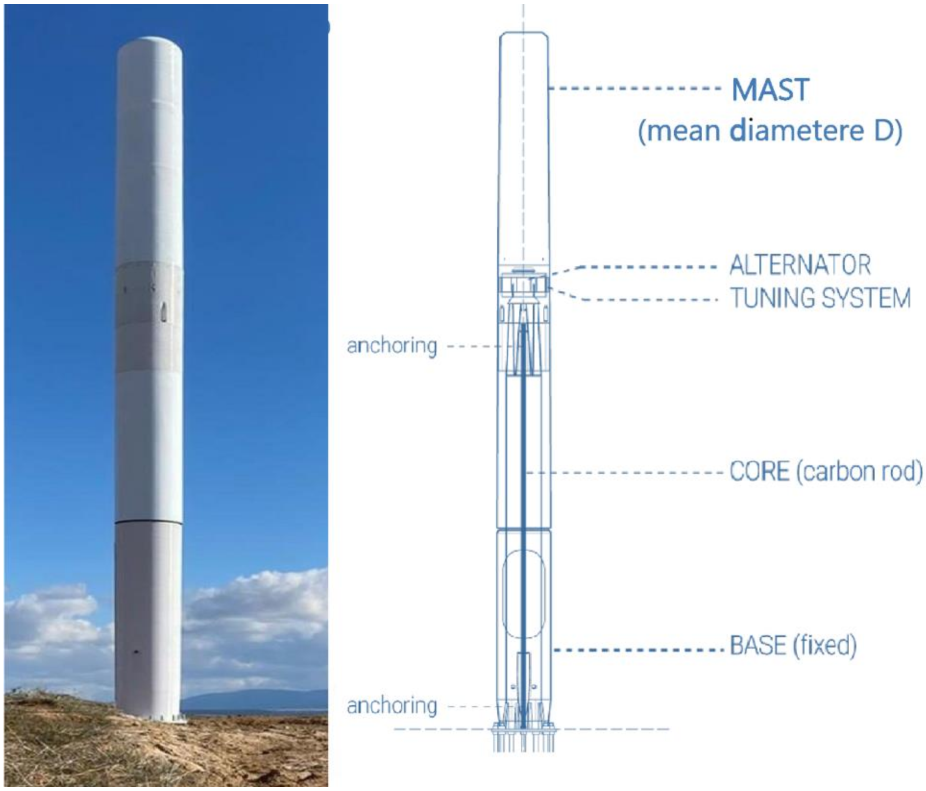

Fig. 1. Vortex bladeless generator model [1].

Normally, the flow pattern is described by two turbulent shear layers on both sides of the mast [2].

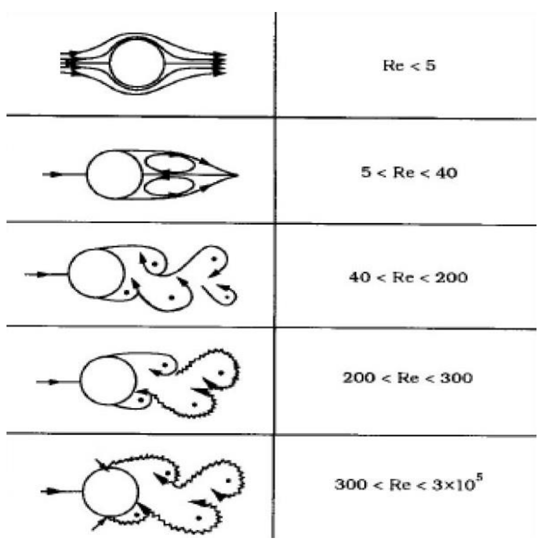

Fig. 2. Schematic of vortices behind a circular cylinder at different Reynolds numbers [3].

The shedding vortices behave periodically with a frequency of f_T. This frequency is related to the air velocity U and the size of mean diameter D, which define the Strouhal number as follows [3]:

$$St = f\frac{D}{U} \tag{1}$$

As the Reynolds number is raised from zero, the oscillation frequency increases. A Reynolds number exists at which the vortex shedding frequency and the body's natural frequency are close. Thus, with the low range of mechanical properties and mass, significant oscillation can be transversed to the bladeless turbine. When the bladeless generator oscillates, a complicated interaction is created between the mast and air. Two critical parameters must be outlined: the size of a mean diameter (D) that makes the generator's natural frequency synchronize with the vortex shedding frequency (lock-in regime) and the generator response indicated with the amplitude of the top of the mast.

The idea of using vortex-induced vibration (VIV) for harnessing energy was first used by Bernitas [4], who made a device called VIVACE (Vortex Induced Vibration Aquatic clean energy). This device uses the VIV energy with a circular cylinder mounted on a spring in a different flow velocity to harvest electricity. Other approaches have been recently analyzed by Barrero-Gill [5] and Q.Zhu [6]. Rostami et al. investigated the analytical solution of vortex-induced vibration [3]. One precise model of a vortex bladeless wind turbine consists of the forced oscillation of the structure exposed to the fluid flow domain accomplished by the Navier-stocks equations, considering dynamic boundaries [7]. Considering all the complications related to the modeling fluid flow, a two-dimensional flow model exerting a crosswise lift force on both sides of the mast is recommended. With this model [8], semi-empirical methods [9] or analytical methods [10] replace the sophisticated CFD calculations. Considering the complications of CFD and analytical simplifications, semi-empirical models are more favorable. The most conventional semi-empirical model of the vortex-induced vibration force is the method of a wake vibration with a variable flow that models vortex shedding, which is harmonic [11]. The flow should satisfy the van der Pol equation, which results in a harmonic and stable vibration [12]. The model of a semi-empirical wake oscillator has been demonstrated to have the potential to clarify basic features of VIV, such as the lock-in phenomenon and limit cycle oscillations [13]. Because of the structural forced oscillations, modeling of vortex-induced vibration bladeless wind turbines is complicated and leads to PDEs (partial differential equation). These equations can be reduced with various approaches, such as the Galerkin method, and turned into ODEs (ordinary differential equations) [7]. Other techniques are proposed to simplify the structural oscillation model, such as the method of lumped parameters [14, 15], Rayleigh-Ritz method [16], assumed modes method [17], collocation method [18], and least squares method [19]. In this paper, to calculate the most optimum mechanical properties, the mass-damping parameter ($m^*\zeta$) is used to maximize the efficiency of the vortex bladeless generator with analytical methods followed by verification of the results with a numerical solution.

2. Efficiency of vortex bladeless generator

2.1. Mathematical model for optimizing vortex bladeless generator

A circular cylinder mounted on a spring is used as a simplified vortex bladeless generator. This model is recommended in several VIV studies. The mass oscillates in the y direction, as shown in Figure 3, and has a natural frequency of oscillation f_n and a mass per unit length m. Air forces on carbon fiber rods are neglected, considering the small diameter.

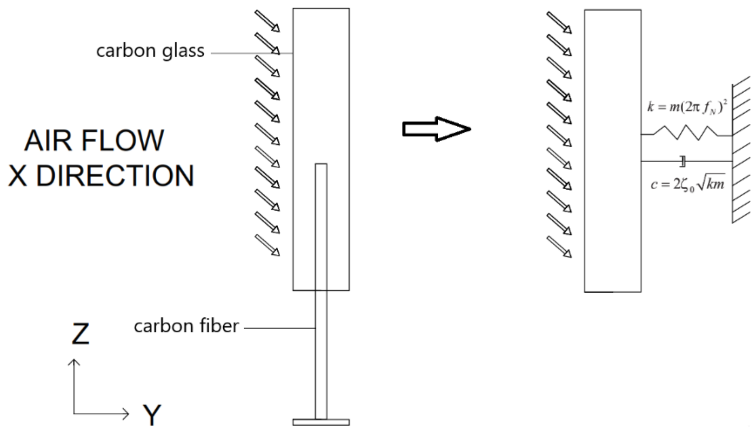

Fig. 3. Simplified model for vortex bladeless generator with a mast of length 1 m

Some important parameters to simulate the bladeless generator as a spring-mounted circular cylinder are the mass ratio m* (the dimensionless number that is defined as the ratio of the mean density of the mast to the density of the air), the reduced velocity U* (the dimensionless number that is defined as the ratio of convective acceleration to the local acceleration of the flow), the mechanical damping ζ, the Reynolds number Re, or the aspect ratio L/D (see Figure. 3). Additionally, it is of interest to find how the energy efficiency depends on these parameters. The main goal of this paper is to study the role of the mean diameter and mechanical-damping parameter (m*, ζ) in the energy efficiency for the simplified form of a vortex bladeless generator.

The equation that governs the transversal displacement of the mast is as follows [20]:

$$\boldsymbol{m(\ddot{y} + 2\zeta\omega_n\dot{y} + \omega_n{}^2 y) = F_y(t)} \quad (2)$$

where the dot denotes the time derivative.

An experimental study carried out by Hovar [20] shows that the Lock-in region can be approximated by an air force per unit length using Equation (3) [20].

$$\boldsymbol{F_y = \frac{1}{2}\rho U^2 D C_y(t) = \frac{1}{2}\rho U^2 D C_y sin(2\pi f t + \phi)} \quad (3)$$

where ϕ is the phase angle that forces drive the cylinder to the direction of displacement and f is the vibration frequency [17]. Substituting Equation (2) in Equation (3), considering (according to experimental data) a steady state of harmonic vibrations y(t)=A sin(2πft), and regarding sine and cosine terms, the equation for the normalized frequency f* = f/fn and normalized amplitude A* = A/D is [20]:

$$f^* = \frac{f}{f_n} = \left(1 - \frac{C_y\, cos\phi U^{*2}}{8\pi^2 m^* A^*}\right)^{\frac{1}{2}} \tag{4}$$

$$A^* = \frac{A}{D} = \frac{C_y\, sin\phi}{16\pi^2 m^* \zeta}\left(\frac{U^{*2}}{f^*}\right) \tag{5}$$

As it can be concluded from Equations (4) and (5), A* is a function of two parameters, m* and ζ, as well as U*, that are independent.

2.2. The efficiency of vortex bladeless generator

The energy efficiency can be considered over one cycle of oscillation (T) by the amount of work done per unit length by the air. Therefore, the efficiency factor is defined by the ratio of the mean power imposed to the body by the flow per unit length P_{F-B} and the total power that exists in the flow per unit length P_F, that is [20]:

$$\eta = \frac{P_{F-B}}{P_F} \tag{6}$$

Considering the total power per unit length in the flow given in Equation 7. The power imposed on the body per unit length and the cycle of oscillation T from the flow by the oscillating body is given by [20]:

$$P_F = \frac{\rho U^3 D}{2} \tag{7}$$

$$P_{F-B} = \frac{1}{T}\int_0^T F_y \dot{y}\ dt \tag{8}$$

According to sinusoidal vibrations in the steady state flow with amplitude A and frequency f, it follows from Equations (3) and (8) that the efficiency factor can be defined in terms of the normalized velocity, amplitude, and frequency. In the experimental study which gives the excitation coefficient CYsinϕ, (Equation 9) [20], the efficiency factor is defined as:

$$\eta = \pi A^* C_y sin\phi \left(\frac{f^*}{U^*}\right) \tag{9}$$

Equation 9 should be calculated for the best efficiency at the design stage. Experimental data that have been extracted by Hovar [20] were used to have $C_y sin\phi$ and$C_y cos\phi$.

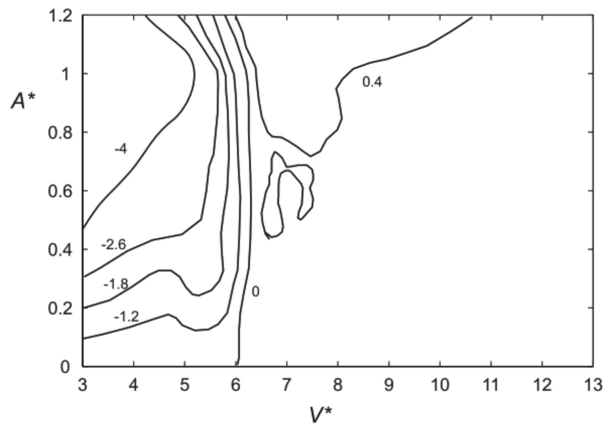

Fig. 4. Contour plot of CYsin**ϕ** measured by Hover et al. [20].

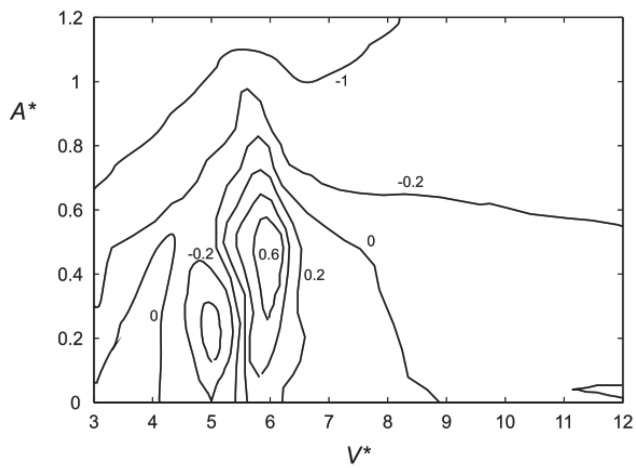

Fig. 5. Contour plot of CYcos**ϕ** measured by Hover et al. [20].

Four steps have been taken to calculate efficiency:

The amplitude of true reduced velocity V* (that is fixed) is chosen according to the environment where the generator will be installed.

The normalized amplitude and frequency increase from 0 to 1 and 0.5 to 1.5 until Equations (4) and (5) are satisfied. Two residuals are defined (Equations (10) and (11)):

$$\boldsymbol{res1_i = A^* - \frac{C_y\, sin\phi}{16\pi^2 m^* \zeta}\left(\frac{U^{*2}}{f^*}\right)} \tag{10}$$

$$\boldsymbol{res2_i = f^* - (1 - \frac{C_y\, cos\phi U^{*2}}{8\pi^2 m^* A^*})^{1/2}} \tag{11}$$

The process continues until both res1i < 0.01 and res2i < 0.01 satisfy.

The actual reduced velocity is changed in a step of 0.1 in the range of 4–14.

3. Results

Math Works MATLAB R2022b is used to calculate efficiency and normalize amplitude, and the results are shown in Figure 6:

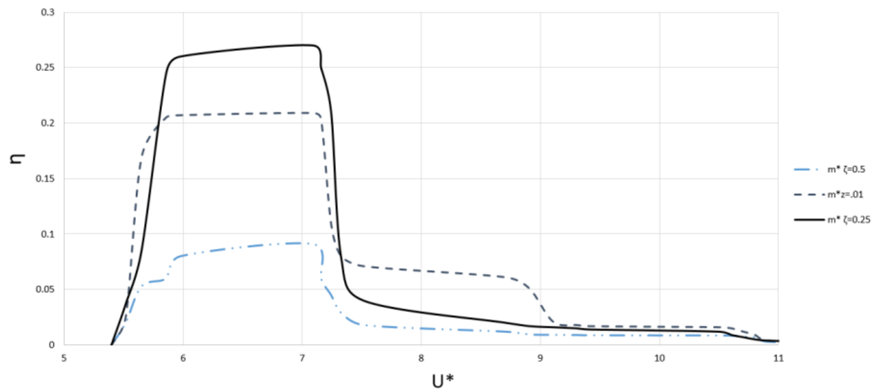

Fig. 6. Energy efficiency for different values of the mass-damping parameter.

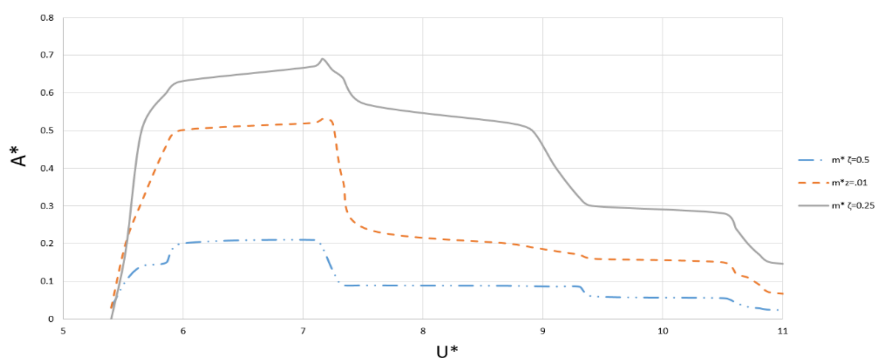

Fig. 6. Normalized amplitude for different values of the mass-damping parameter.

In Figure 6, the efficiency factor η and normalized amplitude are maximum when mechanical properties are around 0.25, and the bladeless generator is expected to have its best performance. The material specifications used for our generator in Table 1 are chosen from Satish Raghuwanshi's study [20].

Using the results and the material specification, the best performance of the Vortex bladeless generator is when the mean diameter of the mast is 0.0984 meters and the reduced velocity is 7.3.

A numerical approach is used to validate these results, which will be discussed in the next section. Normalized amplitude is examined for analytical validation with CFD methods.

Table. 1. Material specification of the mast.

material specification	*Vortex generator*
Young's modulus (GPa)	*3.2*
Mast Length (CM)	*100*
Thickness (mm)	*2.5*
Mast Density (kg/m3)	*1380*

4. Numerical approach and validation

The grid structure and methods used to solve the flow field are briefly explained in this section. The analytical approach is validated with CFD methods in fluent software. The simulation parameters, including grid size and shape, time step size, and CFL number, are calculated fine enough to gain mesh independence and have acceptable errors in turbulent flow simulations [15]. **Q2**

4.1.Grid Structure

The flow domain specification contains a two-dimensional rectangular block of dimensions 35D × 14D. The center of the Vortex bladeless generator of diameter is taken as the origin. The grid region has been made concerning moving parts, and we used a non-deforming grid to produce more accurate results. Grid dependency has been checked in Figure 8. Thus, the resulting grid has 93526 elements and 92826 nodes.

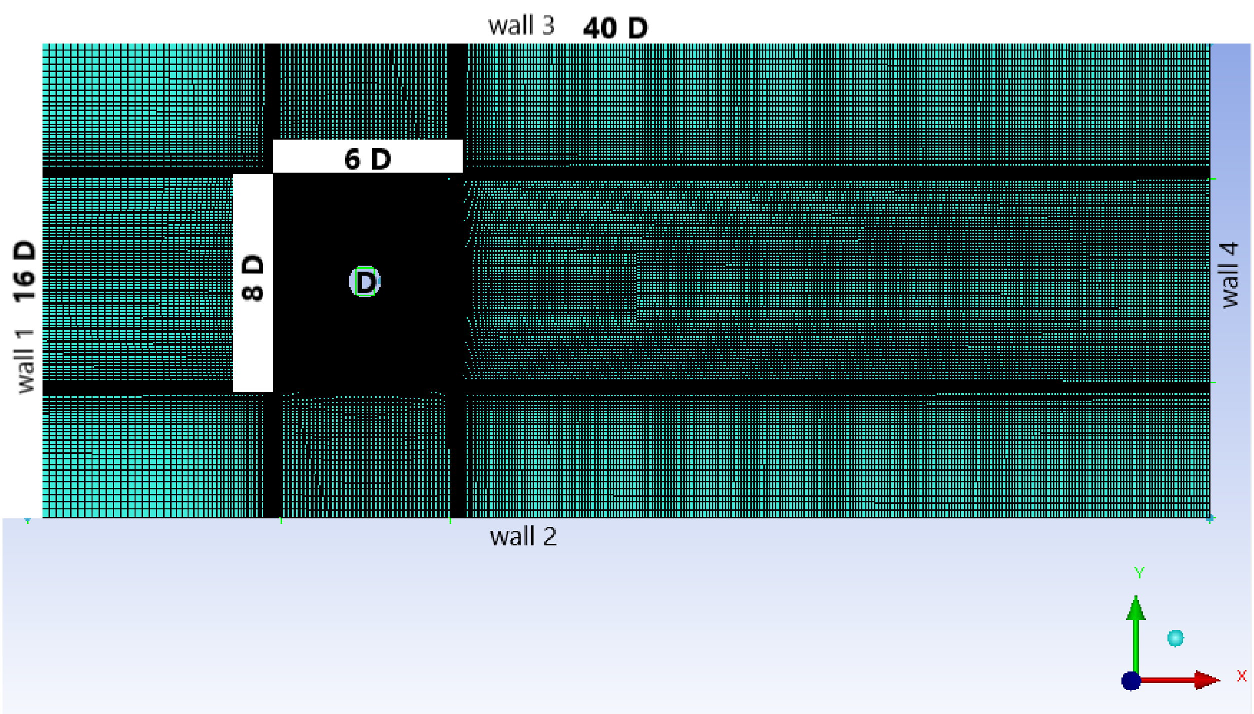

Fig. 7. Computational domain.

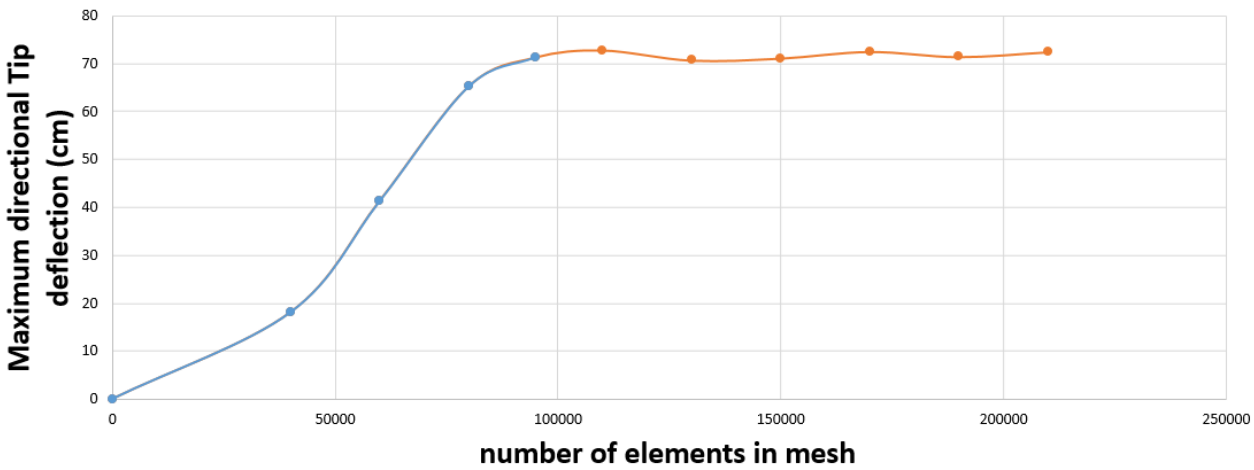

Fig. 8. Grid dependency.

The Reynolds Average Navier Stokes (RANS) model is applied to simulate the turbulent flow. The boundary layer is generated around the mast. Applying the dynamic mesh and using a hybrid grid shape, the flow-induced vibration of the bladeless generator, which moves in the vertical direction of flow, is solved. There are initially a total of 93526 elements in the domain, but this number is prone to changes due to the deformation of elements. As can be seen, the generator is designed to have the best performance when U*=7.24. By knowing the stiffness and natural frequency of the generator, the velocity of the air should be around 6.72 m/s. The function of the spring is defined using a user-defined code (UDF).

4.2. Assumption and boundary conditions:

In this study, the Piso algorithm is applied, which is recommended for VIV problems [14]. Dynamic mesh is activated, and residuals are set to 0.001; the height of the first element is determined to be 0.0025, and the boundary conditions are as follows:

Wall 1 (velocity inlet): 6.72 m/s
Wall 2 & Wall 3: symmetry
Wall 4: pressure outlet

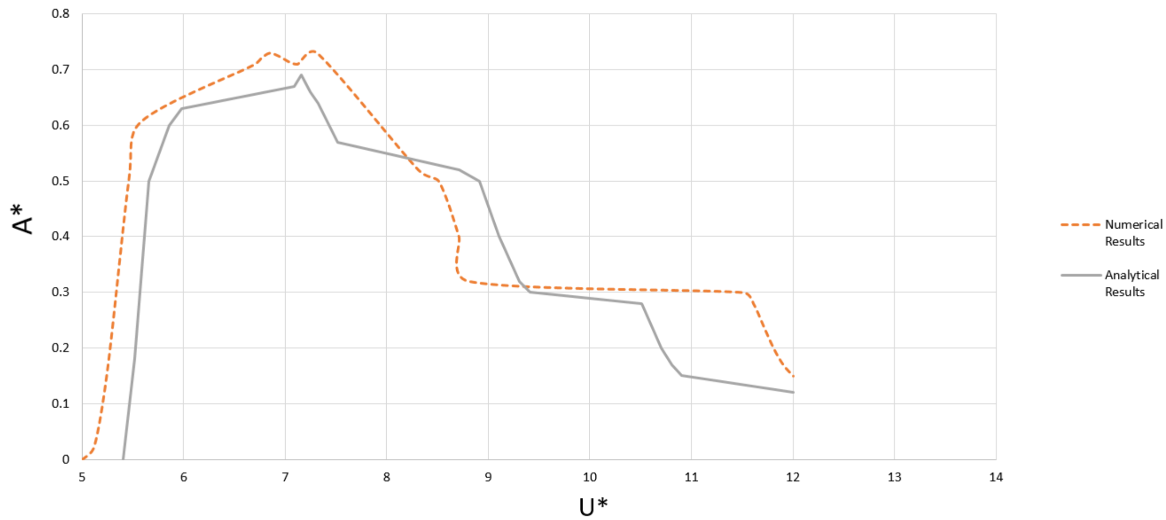

Fig. 9. Normalized amplitude for different values of the mass damping parameter.

As shown in Figure 9, both numerical and analytical results are nearly the same and can be used to simulate the vortex bladeless generators according to installation sight.

5. Conclusions

This paper studied the effect of critical parameters, like mean diameter and mass-damping coefficient, on the efficiency of a vortex bladeless turbine. A mass-spring model is considered to simulate a vortex bladeless turbine. The efficiency factor is defined by the normalized mass, normalized amplitude, normalized efficiency, and reduced velocity. Experimental data is used to calculate the forces that act on the mast. It was shown that the vortex bladeless turbine performs best at a velocity of 6.8 m/s when the mass-damping parameter is around 0.25 and the reduced velocity is 7.3. Thus, the mean diameter of the mast should be around 0.0984 m for the turbine to experience the Lock-in situation. A two-dimensional CFD model is used with transient conditions to validate the analytical approach. The K-ω SST is used. Piso algorithm is applied.
In conclusion, the CFD model has shown an 8% discrepancy from the analytical result, which is an acceptable error. It was indicated that the results presented in this paper could be representative. From an engineering point of view, the parametric analysis of the present study can help to design a device to extract useful energy from VIV efficiently. The experimental prototype has been built and planned to be tested with the parameters found in this study.

References

[1] C.H.K. Williamson, Vortex Dynamics in the Cylinder Wake, Annual Review of Fluid Mechanics, 28 (1996) 477-539.
[2] A. Abdelkefi, Aeroelastic energy harvesting: A review, International Journal of Engineering Science, 100 (2016) 112-135.
[3] A.B. Rostami, M. Armandei, Renewable energy harvesting by vortex-induced motions: Review and benchmarking of technologies, Renewable and Sustainable Energy Reviews, 70 (2017) 193-214.

[4] M.M. Bernitsas, K. Raghavan, Y. Ben-Simon, E.M.H. Garcia, VIVACE (Vortex Induced Vibration Aquatic Clean Energy): A New Concept in Generation of Clean and Renewable Energy From Fluid Flow, Journal of Offshore Mechanics and Arctic Engineering, 130 (2008) 041101.
[5] A. Barrero-Gil, G. Alonso, A. Sanz-Andres, Energy harvesting from transverse galloping, Journal of Sound and Vibration, 329 (2010) 2873-2883.
[6] Q. Zhu, M. Haase, C.H. Wu, Modeling the capacity of a novel flow-energy harvester, Applied Mathematical Modelling, 33 (2009) 2207-2217.
[7] R.A. Skop, S. Balasubramanian, A new twist on an old model for vortex-excited vibrations, Journal of Fluids and Structures, 11 (1997) 395-412.
[8] T. Wu, A. Kareem, Vortex-induced vibration of bridge decks: Volterra series-based model, Journal of Engineering Mechanics, 139 (2013) 1831-1843.
[9] D.J. Olinger, A low-order model for vortex shedding patterns behind vibrating flexible cables, Physics of Fluids, 10 (1998) 1953-1961.
[10] P. Monkewitz, C. Williamson, G. Miller, Phase dynamics of Kármán vortices in cylinder wakes, Physics of Fluids, 8 (1996) 91-96.
[11] R.E.D. Bishop, A. Hassan, The lift and drag forces on a circular cylinder oscillating in a flowing fluid, Proceedings of the Royal Society of London. Series A. Mathematical and Physical Sciences, 277 (1964) 51-75.
[12] M.L. Facchinetti, E. De Langre, F. Biolley, Coupling of structure and wake oscillators in vortex-induced vibrations, Journal of Fluids and structures, 19 (2004) 123-140.
[13] R. Skop, O. Griffin, A model for the vortex-excited resonant response of bluff cylinders, Journal of Sound and Vibration, 27 (1973) 225-233.
[14] S.M. Hasheminejad, M. Jarrahi, Numerical simulation of two dimensional vortex-induced vibrations of an elliptic cylinder at low Reynolds numbers, Computers & Fluids, 107 (2015) 25-42.
[15] W. Thomson, Theory of vibration with applications, CrC Press, 2018.
[16] H.L. Dai, A. Abdelkefi, Y. Yang, L. Wang, Orientation of bluff body for designing efficient energy harvesters from vortex-induced vibrations, Applied Physics Letters, 108 (2016) 053902.
[17] F.M. Besem, J.P. Thomas, R.E. Kielb, E.H. Dowell, An aeroelastic model for vortex-induced vibrating cylinders subject to frequency lock-in, Journal of Fluids and Structures, 61 (2016) 42-59.
[18] R. Sanchez, R. Palacios, T.D. Economon, H.L. Kline, J.J. Alonso, F. Palacios, Towards a Fluid-Structure Interaction Solver for Problems with Large Deformations Within the Open-Source SU2 Suite, in: 57th AIAA/ASCE/AHS/ASC Structures, Structural Dynamics, and Materials Conference, American Institute of Aeronautics and Astronautics, 2016.
[19] L. Song, S. Fu, J. Cao, L. Ma, J. Wu, An investigation into the hydrodynamics of a flexible riser undergoing vortex-induced vibration, Journal of Fluids and Structures, 63 (2016) 325-350.
[20] F. Hover, A. Techet, M. Triantafyllou, Forces on oscillating uniform and tapered cylinders in cross flow, Journal of Fluid Mechanics, 363 (1998) 97-114.